Appendix 1 - Corrosion Properties of ZrTiBe + Me Alloys in HCl

A brief discussion about the mechanical requirements of orthopaedic hardware is presented in section 1.6.1 of the introduction. It was initially thought that many of the newly developed alloys would be ideal for orthopaedic applications from a mechanical point of view and biocompatibility considerations would be the deciding factor in whether or not the alloys could be used as implants. A survey of biocompatibility literature is daunting for a non-biologist. We verified that Ni is not biocompatible [1], but alloys containing Ni such as 316L stainless steel (13 - 15 weight % Ni) and Nitinol (55 weight % Ni) are regularly used in the body [2]. This is a striking example, but many others exist. An article by Burke [3] described 0th order biocompatibility as simply a corrosion phenomenon. If the alloy dissolves in the body then it releases ions and material that may be harmful.

We chose to do a first screening of our alloys for corrosion resistance before delving into biocompatibility. With limited equipment to test corrosion properties in our lab, we chose four highly corrosive solutions, 37% w/w HCl, 50% w/w NaOH, 0.6M NaCl, and 10x PBS, to test the corrosion resistance at 1g alloy to 30 ml static solution of three metallic glass compositions, $Zr_{35}Ti_{30}Be_{35}$, $Zr_{35}Ti_{30}Be_{29}Co_6$, and $Zr_{44}Ti_{11}Cu_{10}Ni_{10}Be_{25}$, and three commonly used alloys for biomedical applications, Ti-6Al-4V, 316L Stainless Steel, and CoCrMo. Mass loss measurements were conducted at 1 week, 1 month, and 3 months and for all solutions except HCl. No mass loss was detectible until the three month time period. Inductively coupled plasma mass spectrometry (ICPMS) measurements were used to analyze the solution for dissolved elements at 3 months. 0.6M NaCl and 10x PBS solutions caused <0.1% mass loss for

each of the alloys after three months and ICPMS revealed no further information because the dissolved material was below the detection limit of the instrument. NaOH results did show minimal mass loss at 3 months and the results are presented in Table A1.1. It was determined that all alloys had excellent corrosion resistance in the tested solutions excluding HCl.

Table A1.1: Mass loss and ICPMS measurements of NaOH solution after 3 months. Solution acidified to 2% w/w HNO3 as required for ICPMS.

Alloy	ZrTiBe	ZrTiBeCo	ZrTiBeCuNi	316L SS	Ti64	CoCrMo
Mass Loss	0.10%	0.10%	0.40%	<0.1%	0.20%	0.10%
Elements of Interest	Be = 75ppb	Be = 60ppb	Be = 400ppb	<50ppb	Al = 50ppb	Co,Cr=100ppb
	Zr = 1ppm	Zr = 1.7ppm	Zr = 15.7ppm		Ti = 200ppb	Mo =200ppb

Corrosion rates in HCl were enormous for most of the alloys tested. $Zr_{44}Ti_{11}Cu_{10}Ni_{10}Be_{25}$ dissolved in under 10 minutes. Most of the other alloys were completely dissolved in 1 week, $Zr_{35}Ti_{30}Be_{35}$ survived for almost 1 month, and the only alloy to survive the full 3 months was CoCrMo which lost 12% of its mass. Corrosion rates in HCl were seen to vary by many orders of magnitude depending on composition. We sought to find the most corrosion resistant BMG for biological applications and given that this was an acidic chloride containing environment, we saw an opportunity to quickly differentiate corrosion resistances in a possibly biologically relevant environment. The information in this appendix is expected to be submitted as a paper entitled, "Corrosion Properties of ZrTiBe + Me Alloys in HCl," with the authors A. Wiest, S. Roberts, M.D. Demetriou, and W.L. Johnson.

A1.1 Abstract

ZrTiBe + Me alloys, where Me is a metallic element, were immersed in concentrated HCl and the corrosion rates were measured. Depending on the fourth

alloying element corrosion rates from 10^2 - 10^7 MPY where MPY = 0.001 in/yr were observed. Corrosion rate and standard half cell potential of the Me element are correlated and show a log linear relationship. Surface chemistry is examined with XPS and reveals a completely oxidized surface for samples left in air and approximately 25% pure metal after 3% mass loss in HCl.

A1.2 Introduction

Zr based bulk metallic glasses (BMG) are often noted for their high corrosion resistance [4-5]. Vitreloy 105 has corrosion rates similar to Ti-6Al-4V, CoCrMo, and 316L stainless steel in phosphate buffered saline solution. In simulated sea water (0.6M NaCl), Vitreloy 105 exhibits corrosion rates comparable to many alloys used in marine environments. The recently published $Zr_{35}Ti_{30}Be_{35}$ and $Zr_{35}Ti_{30}Be_{29}Co_6$ glasses have an order of magnitude higher corrosion resistance than Vit 105 in 0.6M NaCl [6].

The ZrTiBe + Me alloys where Me is an additional metallic element are the subject of this study. The corrosion resistances of the constituent elements in our base ternary alloy have been previously studied. Yau reorted that “titanium is immune to all forms of corrosive attack in seawater and chloride salt solutions at ambient temperatures” in Corrosion Engineering Handbook [7]. Beryllium has been measured in oxygen free and oxygen saturated solutions at 90 °C with NaCl concentrations ranging from 28μM - 0.85M. Low corrosion rates are observed for oxygen free water, however the rate increases by two orders of magnitude in saturated oxygen water [8]. Zr is fully resistant to attack at temperatures up to 100 °C in saturated NaCl [7, 9]. Ti alloyed with >10% Zr is found to be more corrosion resistant in 90% H_2O_2 solutions than pure Ti. Thus it is not surprising our alloys would exhibit high corrosion resistance in NaCl solutions.

In order to differentiate corrosion rates of alloys with high corrosion resistance and attempt to understand the mechanisms of corrosion better, 12M HCl was chosen as an acidic chloride containing environment. Zr has high resistance to corrosion in 12M HCl at room temperature, showing corrosion rates of <0.01μm/yr [9]. Ti and Be are much more susceptible in elemental form to attack in HCl. Corrosion rates spanning 5 orders of magnitude were observed for ZrTiBe + Me glasses containing 1 - 5% of an additional alloying element. Rates depended strongly on the "nobility" or standard half cell potential of the alloying element.

A1.3 Experimental Method

6 - 10g master ingots were arc melted on a Cu hearth under a Ti-gettered argon atmosphere. Alloys were composed of elements >99.9% purity and ingots with more than 0.1% variation in mass before and after melting were discarded. Alloys were cast amorphous into 2 or 3mm diameter rods depending on glass forming ability. Corrosion tests were performed in static solution of 12M HCl in loosely capped high density polyethylene bottles at room temperature using a ratio of 30 mL HCl to 1g alloy. Given the low volume of corrosive media, corrosion rates were calculated using times corresponding to mass losses of 1 - 5%.

Surface chemistry was examined using X-ray photoelectron spectroscopy (XPS). Samples of the same composition were cut from a single rod and polished to 0.05μm surface finish. One sample from each rod was left in air to examine the passive oxygen layer. Other samples were immersed in 12M HCl until 1 - 3% mass loss was achieved. Samples were removed from 12M HCl, rinsed in methanol to minimize oxide growth, and placed in the XPS with less than 120 s of exposure to atmosphere before vacuum

pumping commenced. Final pressures were in the 10^{-8} torr range. Minimal oxide growth is expected on samples immersed in HCl after removal from the corrosive solution.

A1.4 Results and Discussion

In order to establish a baseline corrosion rate for the ZrTiBe alloys in 12M HCl, Be was fixed at 35 atomic percent and Zr and Ti were varied in 5% increments. Be was maintained at 35% because the best glass forming region in the ternary system is along the Be = 35 line [10]. Figure A1.1 shows the corrosion rates of crystallized $Zr_{25}Ti_{40}Be_{35}$, and amorphous rods of $Zr_{25}Ti_{40}Be_{35}$, $Zr_{30}Ti_{35}Be_{35}$, and $Zr_{35}Ti_{30}Be_{35}$. Note that the corrosion rate decreases as the Zr content of the alloy increases, and the crystalline sample has the fastest corrosion rate. The reason amorphous Zr based alloys exhibit higher corrosion resistance than identical crystalline compositions is not well understood despite other studies observing the same effect [11]. Pd40Ni40P20 shows the opposite effect with the crystalline alloy exhibiting higher corrosion resistance [12].

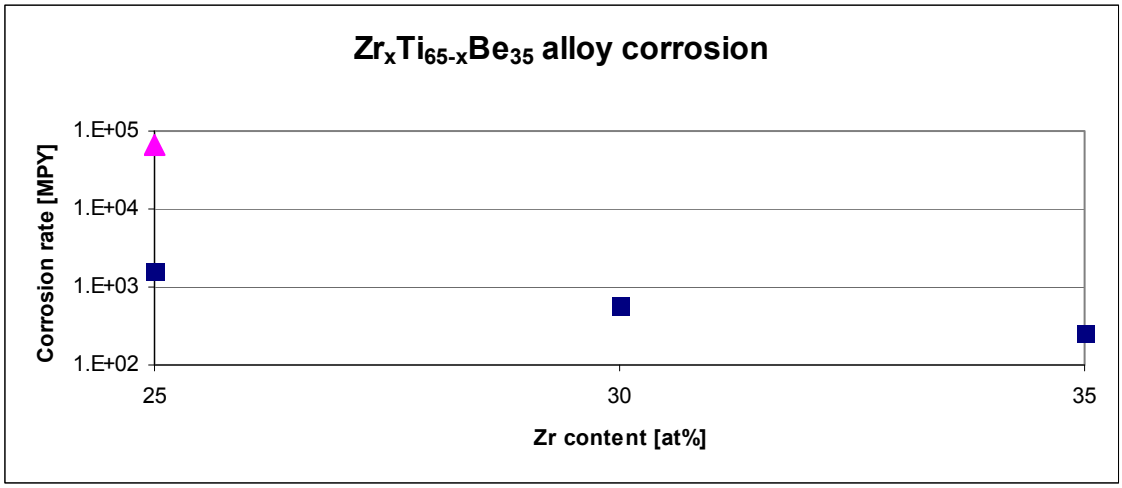

Figure A1.1: Corrosion rate as a function of Zr content in $Zr_{65-x}Ti_xBe_{35}$ alloys. Squares are 2mm diameter amorphous rods. The triangle is a crystallized 2mm diameter sample.

$Zr_{35}Ti_{30}Be_{35-x}Me_x$ alloys, where x ~ 5, were tested in concentrated HCl. Large variations in corrosion rates were measured between different Me additions. Table A1.2 lists the alloys tested and their observed corrosion rates. Figure A1.2 plots standard half cell potential as measured against standard hydrogen electrode (SHE) of the fourth alloying element versus corrosion rate of the alloy in 12M HCl. If the Pd point is omitted, there is a nearly log linear relationship between corrosion rate and the standard half cell potential of the fourth element. With little reason to expect a log linear relationship, one can say that corrosion rate increases as nobility of the fourth alloying element increases. We see the alloy containing Al with a half cell potential E^0 = -1.66V has the lowest observed corrosion rate = 56 MPY while alloys with Pd (E^0 = 0.915V) dissolve so quickly and violently that estimations of corrosion rate = 10^7 MPY are done because complete dissolution happens in under 60 s. The $Zr_{35}Ti_{30}Be_{30}Cu_5$ alloy also exhibits very high corrosion rates = $5*10^4$ MPY.

Table A1.2: Alloy compositions and corrosion rates measured in 12M HCl.

Sample	Corrosion rate [MPY]
$Zr_{35}Ti_{30}Be_{35}$	2.6E+02
$Zr_{30}Ti_{35}Be_{35}$	5.8E+02
$Zr_{25}Ti_{40}Be_{35}$	1.6E+03
$Zr_{25}Ti_{40}Be_{35}$ crystallized	6.7E+04
$Zr_{35}Ti_{30}Be_{30}Al_5$	5.6E+01
$Zr_{25}Ti_{40}Be_{30}Cr_5$	4.3E+02
$Zr_{35}Ti_{30}Be_{29}Fe_6$	7.9E+02
$Zr_{35}Ti_{30}Be_{29}Co_6$	1.8E+03
$Zr_{35}Ti_{30}Be_{27.5}Ni_{7.5}$	2.5E+03
$Zr_{35}Ti_{30}Be_{30}Cu_5$	4.2E+04
$Zr_{35}Ti_{30}Be_{31}Ag_4$	6.4E+04
$Zr_{35}Ti_{30}Be_{31}Pd_4$	1.0E+07

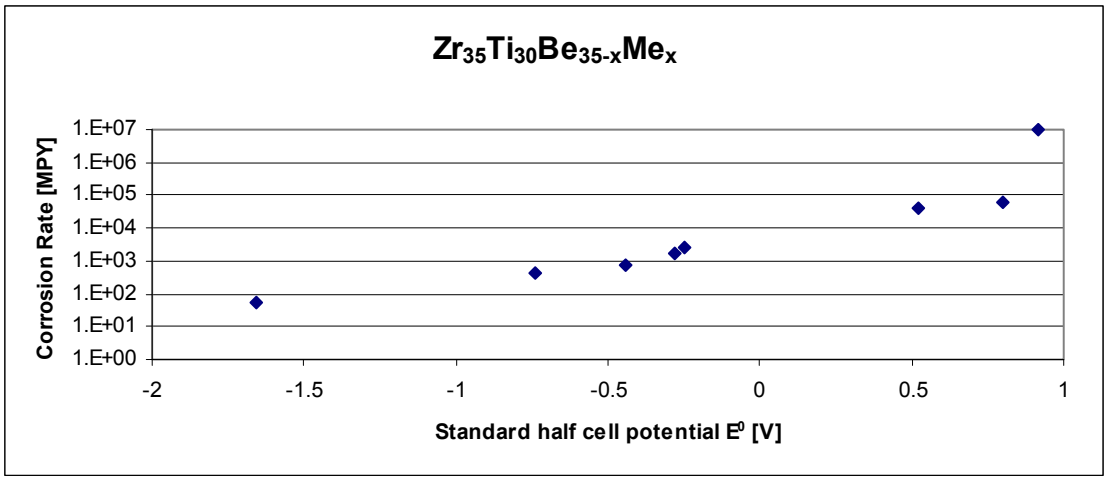

Figure A1.2: Plot of corrosion rate versus standard half cell potential E^0 of quaternary alloying element. Table A1.2 gives compositions.

After immersion in HCl the alloy containing copper had chunks of Cu loosely adhered on the surface, particularly at the ends of the rod. Pitting corrosion was evident over the entire surface of rods removed from the HCl solution, but rods decreased uniformly in diameter and length if pit depth is neglected. Elemental Zr is known to have high corrosion rates in $CuCl_2$ and $FeCl_3$ solutions [9], but the measured corrosion rates for $Zr_{35}Ti_{30}Be_{29}Fe_6$ = 785 MPY and $Zr_{35}Ti_{30}Be_{30}Cu_5$ = 42000 MPY differ by 2 orders of magnitude. The corrosion rate may be somewhat accelerated due to the presence of dissolved Cu or Fe in the acidic chloride solution, but the nobility of the alloying element seems to be a more dominant effect. Given that Cu plates back onto the glass after dissolving into the solution, it may be beneficial to think of the corrosion process in terms of a redox reaction. Zr, Ti, and Be are all anodic elements with tough oxides, giving good corrosion resistance in many environments. When an anodic element is placed next to a cathodic element, the driving force to dissolve the anodic element is proportional to the difference in standard half cell potentials at standard conditions. Since Zr, Ti, and Be have similar half cell potentials, this difference in potential between neighbors would be

mostly dependent upon the Me added. 12M HCl is far outside standard corrosion conditions, and driving force does not predict corrosion rate, but the trend toward higher corrosion rate in alloys with large differences in standard half cell potentials of the elements suggests that the redox driving force may be an important part of the corrosion physics.

XPS was used to analyze the surface chemistry of $Zr_{35}Ti_{30}Be_{35}$. A polished sample left in air for 24 hours showed a fully oxidized surface. Clear oxide peaks for the ZrO_2 3d3/2 and 3d5/2 doublet and the TiO_2 2p1/2 and 2p3/2 peaks along with a weak BeO 1s peak were detected. Peak fitting and integration of the area determined the surface composition to be approximately $(ZrO_2)_{42}(TiO_2)_{25}(BeO)_{33}$. Another sample from the same rod was immersed in 12M HCl for 1 minute and then rinsed in methanol and quickly loaded into the XPS to minimize oxide growth. The surface composition was found to be $(ZrO_2)_{45}(TiO_2)_{24}(BeO)_{31}$. These surface compositions are quite similar and different from the bulk sample composition. Ti and Be are slightly deficient in the surface with Zr dominating the chemistry. It appears that 1 min in HCl is not long enough to alter the surface chemistry of this alloy. Another sample was polished and immersed in 12M HCl for 12 hours resulting in 3% mass loss. This sample was rinsed in methanol and quickly placed in the XPS to minimize time for oxide growth in air and a new surface chemistry was observed. Zr and Ti peaks were visible separate from the oxide peaks and accounted for approximately 25% of the surface chemistry. Figure A1.3 shows the Zr and Ti oxide peaks for the sample left in air and the oxide + metallic peaks for the sample immersed in HCl for 12 hours. Despite 3% mass loss, the oxide is still the dominant surface feature of the sample.

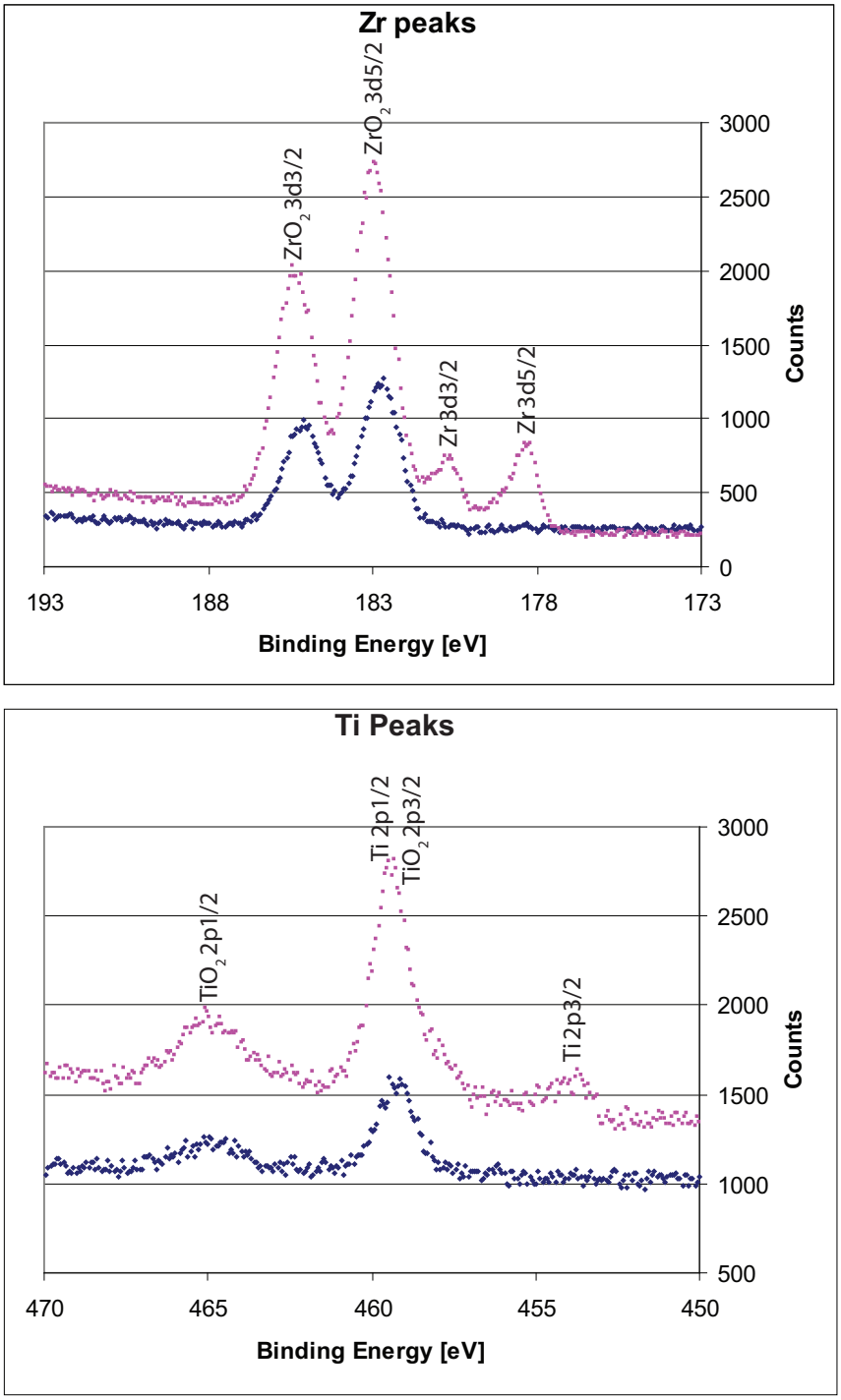

Fig A1.3: High resolution XPS scans of $Zr_{35}Ti_{30}Be_{35}$ after sitting in air for 24 hours (blue) and after being immersed in 12M HCl for 12 hr resulting in 3% mass loss (pink).

A1.5 Conclusion

ZrTiBe alloys are shown to have higher corrosion resistance as the Zr content is increased. A crystallized rod of the $Zr_{25}Ti_{40}Be_{35}$ composition exhibits much higher corrosion rates than the glassy rods. Corrosion rates from 56 MPY to 10^7 MPY are observed when approximately 5% of a metallic element is substituted for Be in $Zr_{35}Ti_{30}Be_{35}$ compositions. The Log of the corrosion rate seems linearly correlated with standard half cell potential or nobility of the alloying element where, counterintuitively, more noble elements cause higher corrosion rates. XPS reveals a completely oxidized surface with surface chemistry differing from the bulk alloy. After dissolution in HCl resulting in 3% mass loss, the surface reveals approximately 25% of the metal is in the unoxidized state.

Appendix 1 References

[1] M. Uo, F. Watari, A. Yokoyama, H. Matsuno, T. Kawasaki, Biomaterials 20 (1999) 747.

[2] J.F. Burke, P. Didisheim, D. Goupil, J. Heller, J.B. Kane, J.L. Katz, S.W. Kim, J.E. Lemons, M.F. Refojo, L.S. Robblee, D.C. Smith, J.D. Sweeney, R.G. Tompkins, J.T. Watson, P. Yager, M.L. Yarmush, in: B.D. Ratner, A.S. Hoffman, F.J. Schoen, J.E. Lemons (Eds.), Biomaterials Science: An Introduction to Materials in Medicine, Academic Press, California, 1996, pp. 283-297.

[3] G.L. Burke, Can. Med. Assoc. J. (1940) 125.

[4] M.L. Morrison, R.A. Buchanan, P.K. Liaw, B.A. Green, G.Y. Wang, C.T. Liu, J.A. Horton, Mater. Sci. Eng. A 467 (2007) 198.

[5] M.L. Morrison, R.A. Buchanan, R.V. Leon, C.T. Liu, B.A. Green, P.K. Liaw, J.A. Horton, J. Biomed. Mater. Res. Part A 74A (2005) 430.

[6] A. Wiest, G.Y. Wang, L. Huang, S. Roberts, M.D. Demetriou, P.K. Liaw, W.L. Johnson, Scripta Mater. in review.

[7] T.L. Yau, in: P.A. Schweitzer (Ed.), Corrosion Engineering Handbook, Marcel Dekker, Inc., New York, 1996, pp. 158-163, 195-252.

[8] J.L. English, in: D.W. White, J.E. Burke (Eds.), The Metal Beryllium, The American Society for Metals, Ohio, 1955, pp. 533-548.

[9] L.B. Golden, in: Zirconium and Zirconium Alloys, The American Society for Metals, Ohio, 1953, pp. 305-326.

[10] A. Wiest, G. Duan, M.D. Demetriou, L.A. Wiest, A. Peck, G. Kaltenboeck, B. Wiest, W.L. Johnson, Acta Mater. 56 (2008) 2625.

[11] S. Hiromoto, A.P. Tsai, M. Sumita, T. Hanawa, Corros. Sci. 42 (2000) 1651.

[12] Y.F. Wu, W.C. Chiang, J. Chu, T.G. Nieh, Y. Kawamura, J.K. Wu, Mater. Lett. 60 (2006) 2416.